

Manipulation and Characterization of a Novel Titanium Powder Precursor for Additive Manufacturing Applications

Y.Y. SUN,^{1,3} S. GULIZIA,^{2,4} C. H. OH,² C. DOBLIN,² Y. F. YANG,¹ and M. QIAN^{1,5}

1.—School of Aerospace, Mechanical and Manufacturing Engineering, Centre for Additive Manufacturing, RMIT University, Melbourne, VIC 3001, Australia. 2.—Commonwealth Scientific and Industrial Research Organisation (CSIRO), Manufacturing Flagship, Clayton, Melbourne, VIC 3168, Australia. 3.—e-mail: yingying.sun@csiro.au. 4.—e-mail: stefan.gulizia@csiro.au. 5.—e-mail: ma.qian@rmit.edu.au

Lowering the cost of feedstock powder has been a major issue for wider applications of additive manufacturing (AM) of titanium (Ti) and its alloys. A novel and inexpensive Ti sponge material was selected as a precursor and processed using a CSIRO proprietary powder manipulation technology (PMT). The manipulated powder was characterized in terms of the particle size distribution (PSD), roundness, flowability in the Hall Funnel flowmeter, static angle of repose (AOR), apparent density and tap density. In addition, a universal powder bed (UPB) system was used to characterize the manipulated powder behavior after raking. Two benchmark powders, virgin Arcam Ti-6Al-4V powder and used Arcam Ti-6Al-4V powder, were assessed for a comparison. PMT processing of the Ti powder precursor produced near spherically shaped Ti powder in the size range of 75–106 μm , which performed very similarly to the used Arcam powder in the UPB system. The CSIRO PMT offers a cost-effective manipulation process to produce Ti powder promising for AM applications, while the UPB system allows a quick assessment of the powder spreading behavior in AM processes.

INTRODUCTION

Titanium (Ti) and its alloys are advanced structural materials that have found important applications in aerospace, medical implantation, chemical processing, marine engineering, desalination, and other industries. However, the high cost of Ti components, arising from both the Ti metal itself and the manufacturing process, hinders their widespread use in these industries.¹ Hence, lowering the cost of the feedstock material and employing near-net-shape technologies are both highly desirable.

In recent years, additive manufacturing (AM), as opposed to conventional subtractive manufacturing, has been recognized as a revolutionary group of near-net-shape fabrication technologies. For powder-based AM techniques, controlled by computer-aided design (CAD) models, feedstock materials are deposited onto a platform and directly melted by a high-energy beam (laser, electron, or plasma beam), leading to the geometry buildup of a part layer by

layer.^{2,3} This technology offers many design and manufacturing advantages including short lead time, high material use efficiency, and ability to build complex and internal features and structures.

The development of AM technologies such as powder-bed fusion processes based on selective laser melting (SLM) or electron beam melting (EBM) has broadened the markets of Ti materials in aerospace, defense, and biomedical implant applications, which require small quantities of functional prototypes and structural components in complicated geometries.^{4–6} Ti-6Al-4V (wt.%) components or samples built by SLM (subject to heat treatment) or EBM are near fully dense and show comparable strength and elongation properties to their wrought counterparts.^{5,7–10} The properties of additively manufactured parts are strongly affected by process parameters including the laser/electron beam power, spot size, scanning speed, and preheat temperature.^{2,7,8,11–15} However, not only the process parameters but also the feedstock powder play a

significant role in determining the properties of the built-up components. For instance, the morphology, particle size distribution, and purity of powders affect the flowability and powder bed formation, and hence the development of melt pools and microscopic homogeneity.^{16–18}

Because of the requirements of spherical morphology, specific particle size ranges and chemical purity, Ti powders used for SLM and EBM processes in the current market are mainly produced by gas atomization (GA) or the plasma rotating electrode process (PREP), both of which have a high operating cost. Furthermore, some AM equipment vendors make available their own proprietary set of powders for their specific machines. As a result, the costs of powders and finished parts are high for the majority of AM operations and applications. For wider applications of Ti AM, cost-effective spherical Ti powders suitable for AM are needed. Much effort is being made in this regard, and examples include the following:

- AMETEK, Inc. (Berwyn, PA)¹⁹ combined the hydride-dehydride (HDH) powder manufacturing process with a secondary plasma process and developed an alternative high-volume, competitively priced, spherical Ti powder production process.
- Withers et al.²⁰ combined a plasma-transferred arc melter with a gas blowing system and produced spherical Ti alloy powders, the cost of which is only three to five times the basic cost of the feeds which is 1/10 to 1/15 times less than current commercial cost of spherical Ti alloy powder.
- Lu et al.²¹ applied fluidized bed jet milling to crushed Ti alloy scraps less than 300 μm and produced microfine high Nb-containing TiAl alloy powders with a mean particle size of 5.32 μm and a Wadell's sphericity factor of 0.820.

The Arcam GA Ti-6Al-4V powder (Arcam, Mölndal, Sweden) is currently the most suitable Ti powder for the Arcam EBM system and has been used as a benchmark for other metal powders. Virgin Arcam Ti-6Al-4V powder can be used many times for AM by EBM. Hence, reusable Arcam Ti-6Al-4V powder can serve as a benchmark too, especially for the development of lower cost Ti powders.

In this study, a novel Ti precursor was selected and manipulated using a CSIRO proprietary powder manipulation technology (PMT) in an attempt to produce lower cost Ti powders for AM. The precursor was produced using a continuous Kroll process developed at CSIRO for the direct production of Ti powder. The CSIRO PMT processed the precursor powder in deionized water mechanically by introducing high shear force. The particle–particle and particle–rotor shaft impact forces contributed to the particle size reduction and spheroidization. The characteristics of the PMT-processed powder were evaluated afterwards. In addition, a universal

powder bed (UPB) system, which was developed by CSIRO and contains an identical powder feed and raking system to that used in an Arcam A1 EBM machine, was applied for the first time to characterize the performance of the PMT-processed Ti powder benchmarked against both virgin and used Arcam Ti-6Al-4V powder.

EXPERIMENTAL METHODS

Powder Source

Two benchmark Ti powders were used: virgin Arcam Ti-6Al-4V powder and used Arcam Ti-6Al-4V powder. The virgin particle size range is quoted as 45–100 μm . According to the results of the particle size distribution of the powders shown in Fig. 1 [which was measured by the laser diffraction method using a Malvern Mastersizer X, Worcestershire, UK], the volume ratio between the 45–75 μm and 75–100 μm fractions is 4 to 3. The recycling of unmelted powder is achieved by using a powder recovery system. The exact number of times the powder had been used was not documented but was more than 30 times, and it is still reusable for part building. The used powder was sieved and particles in the range of 45–106 μm were applied in this study.

Each 30-g batch of as-received novel Ti precursor was processed via PMT processing for 30 min. The particle size distributions for both as-received and PMT-processed powders were analyzed using U.S. Standard Size designated test sieves Nos. 60, 100, 140, 200, 325, and 500, which correspond to sieve openings of 250 μm , 150 μm , 106 μm , 75 μm , 45 μm , and 25 μm , respectively. The sieve column was typically placed in a tapping sieve shaker and shaken for 20 min. Particles from the 45–75 μm and 75–106 μm fractions were mixed together at the ratio of 4 to 3, with the aim of obtaining a similar

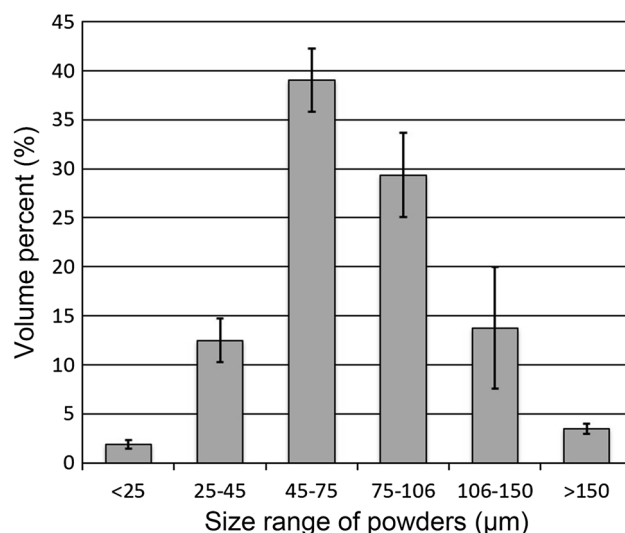


Fig. 1. Particle size distribution of virgin Arcam Ti-6Al-4V powder.

particle size distribution to that of the virgin Arcam powder.

Morphology and Microstructure Analysis

A Phillips XL30 scanning electron microscopy (SEM) system (Philips, Amsterdam, the Netherlands) operating at an accelerating voltage of 5 kV was used to examine the morphology and surface features of both as-received and PMT-processed novel Ti powders at various magnifications. A monolayer of powder was spread on an aluminum sample holder and then coated with iridium to improve sample conductivity and also to promote adhesion of the powder to the tape (preventing the particles from being dislodged once the vacuum system was in operation).

In accordance with ASTM F1877^{7,22} the roundness of both as-received and PMT-processed novel Ti powders was evaluated using a form factor (FF), which is defined as

$$FF = \frac{4A\pi}{P^2} \quad (1)$$

where A is the area enclosed by the boundary of the particle and P is the perimeter of the particle outline. $FF = 1$ corresponds to a perfect circle. High-magnification SEM images were used to calculate the form factors of both powders at different particle sizes. Image Pro Plus 6.0 software (Media Cybernetics, Silver Spring, MD) was used to quantify the area and perimeter of particles by calculating the number of pixels enclosed. The threshold values for each image were adjusted until the particle area appeared completely white and the background appeared completely black. All the complete particles in each image were investigated.

Flowability, Static Angle of Repose, and Density Measurements

Flowability is an important indicator to assess the performance of powder in powder-bed AM systems, and it has a strong influence on the powder layer forming process and hence on the uniformity of the built-up components. Volumetric flowability and static angle of repose (AOR) of both as-received and PMT-processed novel Ti powders were tested. An Arnold meter and Hall funnel were used according to the ASTM B855-06²³ for the volumetric flowability test. This method consisted of slowly sliding a bushing partially filled with powder over a 20-cm³ hole in a hardened steel block. The 20 cm³ of powder obtained after removal of the steel block was transferred to the Hall flowmeter and the flow rate was reported in seconds per 20 cm³. To measure the static AOR, powder was dispensed through a Hall funnel with a 2.5-mm diameter discharge opening onto the center of a horizontal 65-mm diameter plate so that it formed a conical heap. The test was concluded when the powder heap covered

the entire surface of the plate such that further addition of powder would result in no additional accumulation of powder onto the heap. The AOR was then measured as the angle between the surface of the powder heap and the surface of the plate. This procedure was repeated five times and the average values were reported. To exclude the influence of moisture on flowability measurements, powders and devices were dried in a vacuum oven at 80°C for 8 h, and tests were conducted in a fume cupboard immediately after taking them out of the oven.

The apparent density of powders was measured according to the ASTM B703-05.²⁴ A hardened steel block with a 20-cm³ hole was put on a preweighed paper. A bushing partially filled with powder was slowly slid over the hole without tipping, and then the powder was collected and weighed. The apparent density was calculated from the ratio of powder mass and 20 cm³ volume.

The tap density of powders was measured according to the ASTM B527-06.²⁵ Two glass cylinders, 100 mL and 25 mL, were used separately based on the tested apparent density. The cylinders were placed on a tapping apparatus (EU 42E2/110S; J. Engelsmann AG, Ludwigshafen am Rhein, Germany) and tapped until no further decrease in the volume of the powder could be seen (approximately 2,400 tappings). The powder volume was read directly from the cylinders. The apparent and tap densities of each powder were measured four times and averaged.

Performance of Powders on Universal Powder Bed System (UPB)

The UPB contained an identical powder bed system to that used in the Arcam A1 EBM machine and was controlled by a Siemens SINUMERIK 808D programmable logical controller (Siemens AG, Berlin, Germany). Both Arcam Ti-6Al-4V powder and PMT-processed Ti powder were spread by raking on the stainless steel base plate (210 mm × 210 mm) of the UPB. The standard raking speed of the Arcam A1 EBM machine, which is 14 m/min (233.33 mm/s), was employed on the UPB. Each powder generated a different surface texture, the layouts of which were investigated by a Pentax K-x digital camera (pixel resolution of 4288 × 2848; Ricoh Imaging Americas Corporation, Denver, CO,) located right above the base plate. Image Pro Plus 6.0 software was used for statistical image analysis to quantify distribution of particles where raised particles reflect light and show higher pixel intensity, whereas the bottom particles show as dark regions. The original photos were converted to gray images, the black and white intensity of each pixel was exported, then three-dimensional (3D) reconstruction was performed using MATLAB software (The MathWorks Inc., Natick, MA) based on the pixel intensity.

RESULTS AND DISCUSSION

Microstructure

Because AM builds up parts by depositing fused powder layers on top of each other, the size of particles should be strictly controlled as the particle size and layer thickness can have a significant impact on the resolution, surface finish, and the formation of voids, and consequently on the properties of the build. Each AM equipment manufacturer specifies a standard of powder that is allowed to be used for each machine model. In the Arcam EBM system, a powder size range of 45–100 μm together with a layer thickness of $\sim 100 \mu\text{m}$ is normally used,²⁶ and recently the layer thickness has been successfully reduced to 50 μm .²⁷ For SLM systems, a better surface finish can be obtained because a smaller size range of powder (25–45 μm) is commonly used.^{28,29} In fact, even finer powder in the size range of 1–10 μm has been applied on EOS SLM (EOS GmbH, Munchen, Germany) to manufacture dental implant materials with optimized surface properties.³⁰

Figure 2 shows the particle size distributions of as-received and 30-min PMT-processed novel Ti powders. About 78% of the as-received powder mass was coarser than 250 μm (sponge-like block materials), while the amount of the powder finer than 75 μm was negligible. After 30-min PMT processing, only 4.6% of the powder mass was still larger than 150 μm . The concentration of 45–106 μm particles, which meet the size requirement for Arcam EBM, was more than 50%. Approximately 30% of the powder was in the range of 1–45 μm , which is appropriate for the SLM system or cold spray process.

SEM images shown in Fig. 3 display the morphologies of virgin Arcam Ti-6Al-4V powder (Fig. 3a) and used Arcam powder (Fig. 3b). The morphologies of as-received novel Ti powder in two

size fractions (45–75 μm and 75–106 μm) are displayed in Fig. 3c and d. Virgin Arcam particles are spherical in shape and have a rather smooth and shiny surface, which contributes to good flowability during spreading on the powder bed and thus produces a homogeneous microstructure. Some tiny satellite particles are attached to the surfaces of the powder particles due to the GA process. However, after having undergone at least 30 cycles of reuse, the used powder contains particles that show noticeable deformations or distortions on their surfaces (Fig. 3b). A small amount of the used powder has been partially melted, and necks between adjacent particles are formed with metallurgical bonds (Fig. 3b). This is normal but not favored by AM. Moreover, the unbonded satellite particles from the GA process were broken away and mixed into the powders during the blasting process in the powder recovery system.

The as-received novel Ti powder particles are irregular in these size ranges, which are expected to lead to poor flowability on a powder bed and consequently can leave large voids and gaps in built parts. After PMT processing, the morphology of the particles was significantly modified. Figure 4 shows SEM images of PMT-processed Ti powders in an array according to particle sizes. Most of the coarse particles (Fig. 4a–c) show a near-spherical shape. As the particle size decreases, however, the degree of sphericity gets worse and particles below 45 μm become essentially flake like (Fig. 4f). These SEM images provide a visual observation of the particle shape, while roundness measurement can provide statistical information regarding the characteristics of the powder shape. Figure 5 presents the roundness results measured according to Eq. 1. The FF values of the 45–75 μm and 75–106 μm size ranges of virgin Arcam powders are 0.97 and 0.98, respectively, indicating a highly spherical shape. Although the shape of some used particles was deteriorated as shown in Fig. 3b, the average FF values of the used Arcam powder still stay as high as 0.95 and 0.93 for 45–75 μm and 75–106 μm powders, respectively, and the standard deviations are negligible. For PMT-processed powder, the FF value of 150–250 μm particles is 0.8. As the particle size decreases, the FF values remain relatively high, around 0.51 and 0.66 for particles in the size ranges of 45–75 μm and 75–106 μm , respectively. In contrast, for the as-received novel Ti precursor, the FF values of the particles in the corresponding size ranges are 0.45 and 0.48, respectively, with large standard deviations, indicating that the shape between individual particles varies considerably. Figure 6 shows typical surface features of the precursor and PMT-processed Ti powders. A rough and porous exterior is shown in Fig. 6a for the precursor powder, which results from the chemical reaction of the novel production process. Such particles can lead to much higher surface friction and poor flowability when deposited on a powder bed. By comparison, the

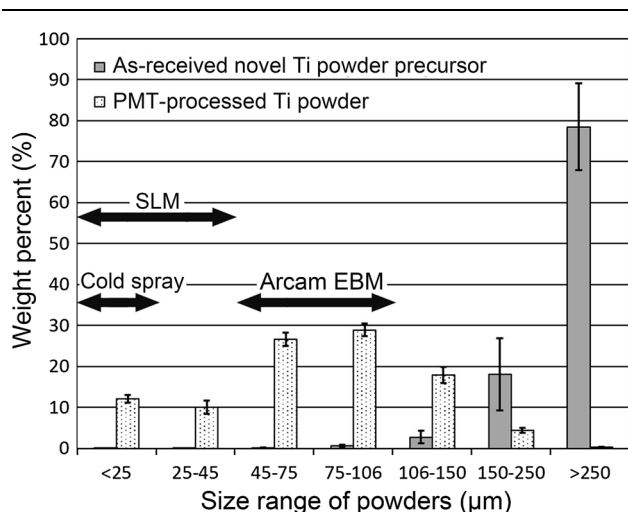


Fig. 2. Particle size distribution of novel Ti powder precursor before and after 30 min PMT processing.

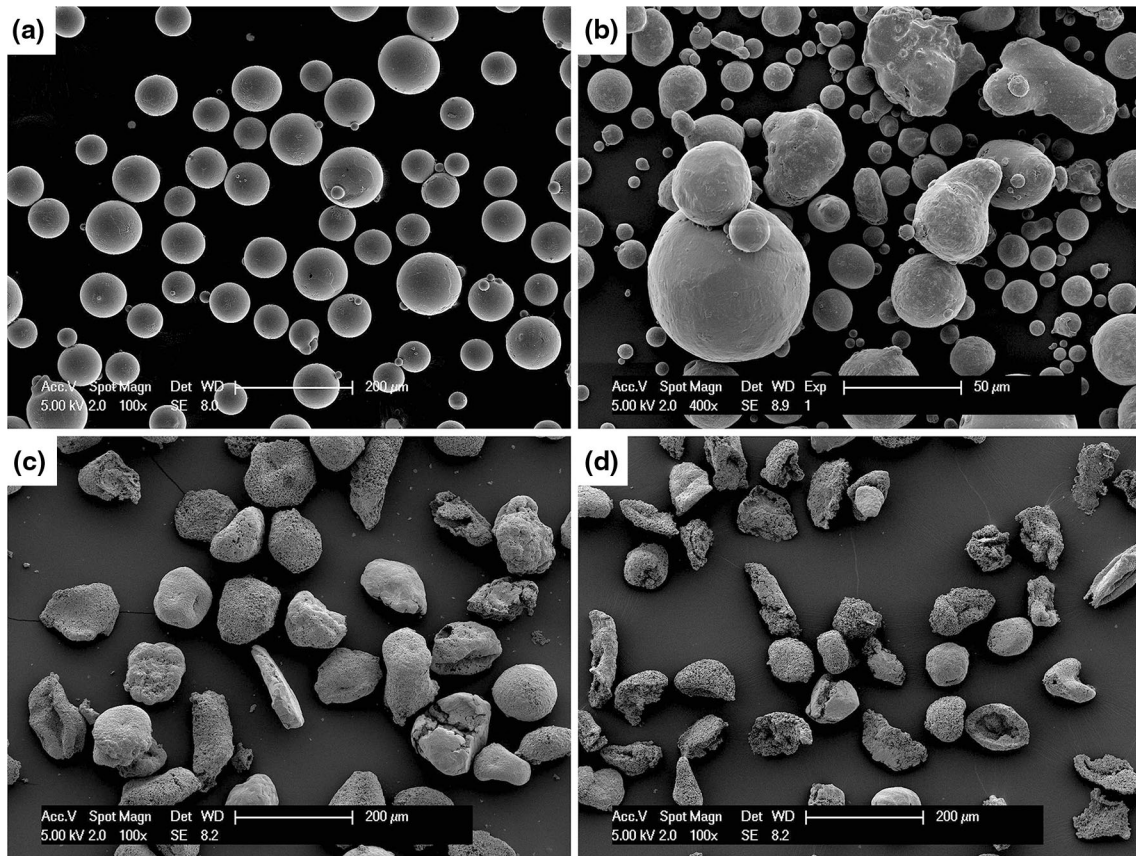


Fig. 3. SEM images of (a) virgin and (b) used Arcam Ti-6Al-4V 45–106 μm powder and (c) 75–106 μm and (d) 45–75 μm as-received novel Ti precursor.

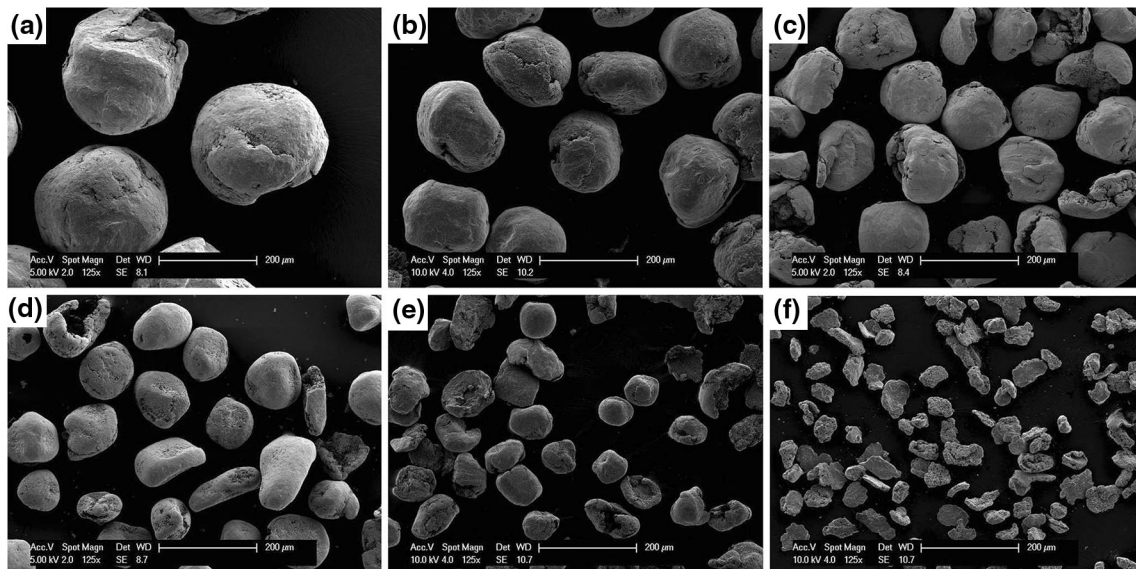


Fig. 4. Morphologies of novel Ti powder after 30 min PMT processing with different particle sizes: (a) > 250 μm , (b) 150–250 μm , (c) 106–150 μm , (d) 75–106 μm , (e) 45–75 μm , and (f) 25–45 μm .

PMT-processed powder shows a relatively smooth and dense surface (Fig. 6b). The formation of this surface can be attributed to the strong particle–

particle collisions and particle–shaft collisions during PMT processing. It should be noted that the interior structure of particles is not affected by PMT

as much as the surface. Figure 6c shows a cross section of a PMT-processed particle that has a dense surface shell but retains a porous interior structure. This internal porosity can be problematic for AM as it may retain this microporosity in the final product. In summary, although the sphericity and surface structure of the resulting powder are not as perfect as the Arcam powder (Fig. 3a), the PMT does effectively break large as-received Ti precursor into smaller particles and markedly improves their morphology especially in the size range of 75–106 μm . The PMT-processed Ti powder will be evaluated below.

Flowability and Performance on Powder Bed

A single, reliable, and widely applicable flowability test does not exist because of the wide variety of both granular materials and the influence of handling on the measurement results.³¹ In this study, the flowability of the particles was characterized using a Hall Funnel and the static AOR, together with apparent and tap densities. The results are listed in Table I. Both virgin and used Arcam powders have much better flowability than the PMT-processed Ti particles. The used Arcam powder presents similar flowability in the Hall Funnel test with virgin powder but it shows a slightly higher static AOR. This means that flowability has deteriorated after being used for more than 30 times. This is because the used powder contains a small amount of half-molten and distorted particles (Fig. 3b) resulting from the EBM process. In this study, approximately 0.3 wt.% of the used particles are larger than 100 μm (it should be noted that the quantity of these irregular particles is related to the specific geometry of the parts being produced). After these oversized particles were removed via the sieving process, some distorted particles within 45–106 μm were still left in the powder lot (Fig. 3b).

The increased geometric complexity of particles interferes with particle movement and consequently this will lead to an increase in the static AOR. The apparent densities of the virgin and used Arcam powders are similar, whereas the tap density of the used powder is marginally higher than that of the virgin powder because of the void filling by loose

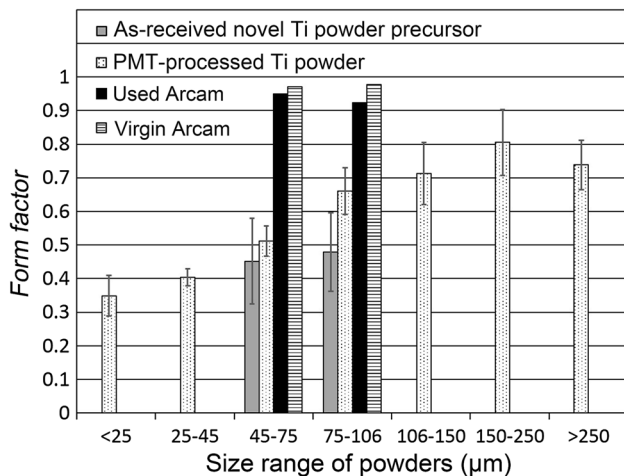


Fig. 5. Roundness comparison among novel Ti powder precursor, 30 min PMT-processed novel Ti powders, and virgin and used Arcam Ti-6Al-4V powders.

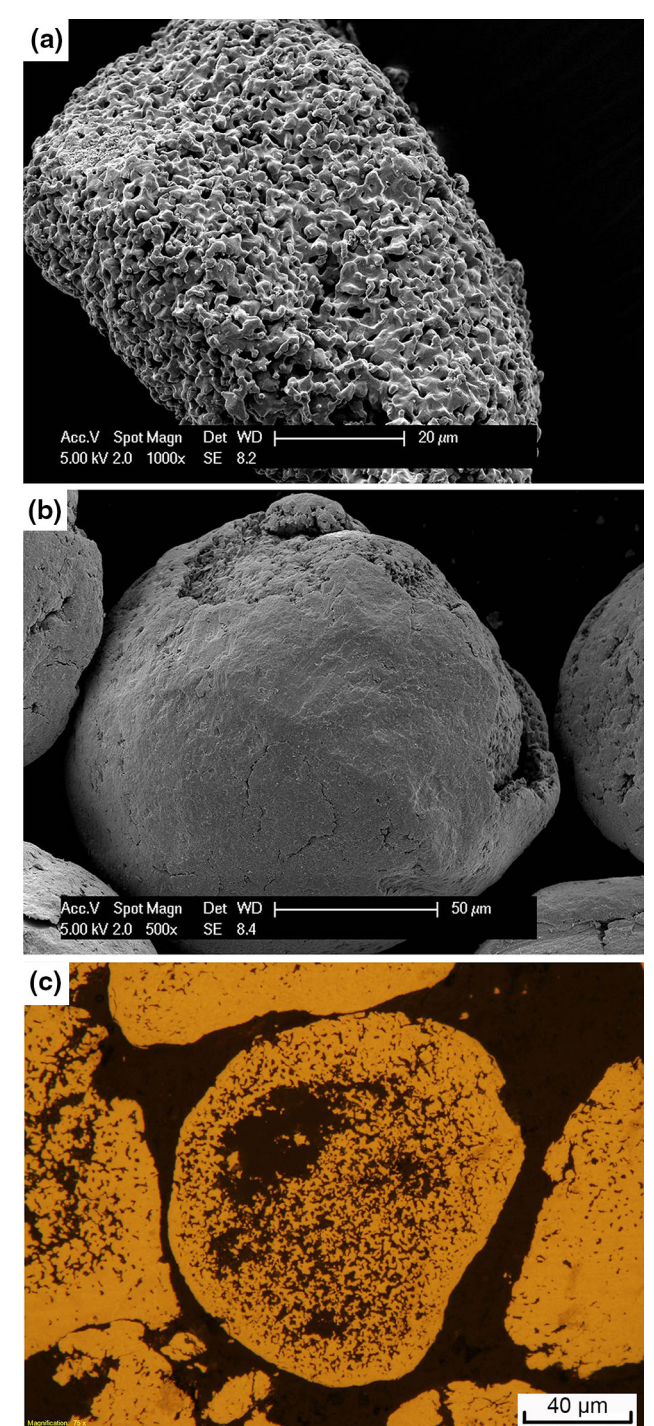


Fig. 6. SEM images showing surface features of novel Ti powder (a) before and (b) after 30 min PMT processing and (c) optical micrograph of the cross-section of a PMT-processed powder particle.

Table I. Flowability, angle of repose, apparent density, and tap density measured for all the powders considered

Powder	Flowability (s/20 cm ³)	Angle of repose (°)	Apparent density (g/cm ³)	Tap density (g/cm ³)
Virgin Arcam Ti-6Al-4V (45–106 μm)	21.3 ± 0.1	32.0 ± 0.2	2.65 ± 0.01	2.87 ± 0.01
Used Arcam Ti-6Al-4V (45–106 μm)	21.4 ± 0.4	35.4 ± 0.9	2.66 ± 0.01	2.94 ± 0.01
PMT-processed Ti 45–106 μm	23.5 ± 0.5	36.0 ± 0.7	1.82 ± 0.01	2.20 ± 0.01
PMT-processed Ti 75–106 μm	23.2 ± 0.5	35.6 ± 0.7	1.72 ± 0.01	2.13 ± 0.01
PMT-processed Ti 45–75 μm	23.8 ± 0.5	36.3 ± 1.2	1.72 ± 0.01	2.04 ± 0.01

tiny particles (Fig. 3b), which were originally present as satellite particles (Fig. 3a).

As the morphology suggested, the PMT-processed Ti powder is not expected to behave as well as virgin Arcam powder, but its performance is acceptable according to Table I. The PMT-processed Ti powder takes only about 2 s longer than the virgin Arcam powder to go through the Hall Funnel and has a static AOR similar to that of the used Arcam powder. Although there is a theoretical density difference between Ti-6Al-4V powder and Ti powder, the influence is expected to be negligible. Due to the decreased roundness, the particles in the range of 45–75 μm behaved slightly worse than those in the range of 75–106 μm in both the Hall Funnel and static AOR tests. Besides, finer particles result in a larger specific surface and, hence, a higher interparticle friction and an increased tendency to absorb moisture from humidity, which also lead to worse flowability. When the particles in these two ranges were mixed together at the volume ratio of 4 to 3, the flowability was slightly deteriorated compared with the 75–106 μm particles. It is likely that small particles can easily wedge themselves into the pores and crevices of coarser particles, thereby affecting the ability of particles to flow relative to one another. The powder layers in the Arcam EBM system are formed by a raking mechanism; therefore, the apparent density plays an important role in the densification of components. The apparent density of virgin Arcam Ti-6Al-4V powder is about 59.4% of the real density (4.43 g/cm³), whereas it is only 40.4% for the PMT-processed Ti powder (compared with the real density of Ti at 4.51 g/cm³). This significant difference is due to the imperfect shape and porous interior structure of particles.

Neither the flowability as tested by the Hall Funnel nor the static AOR can provide a compelling evaluation as to whether a powder is suitable for AM. The most immediate method to test the performance of powder is applying the powder onto a powder bed fusion process. Therefore, the UPB was developed by CSIRO to observe the powder behavior during the raking of the powder bed. On the UPB, a powder spreading system is formed by four rakes with 0.9-mm-wide teeth and 0.1-mm-wide gaps, which interstitially overlap with each other. The powder stocked in two stainless steel hoppers is

gravity fed and the rake fetches the powder. The powder is then raked across the base plate. During particle movement, surface particles will rearrange to a minimum of potential energy under the uniform drive given by the motion of the rake. The kinetic energy of the spreading particles is mostly used to overcome local friction resistances among particles, achieving the minimum energy configuration. Figure 7 shows the surface topographies of five tested powders on the UPB and the corresponding 3D reconstruction profiles of selected areas. With the standard raking speed of 14 mm/min, the most homogeneous spreading surface profile was obtained by virgin Arcam powder (Fig. 7a1–a3). For the used Arcam powder, its surface profile (Fig. 7b1–b3) was largely the same as that of the virgin powder. However, there were some faint rolling tracks distinguishable on the surface (indicated by the broken lines in Fig. 7b1). This is most likely because the small amount of distorted particles remaining in the powder pile prevented the uniform motion of powder during spreading. The difference can also be seen from comparing Fig. 7b3 with Fig. 7a3, in which the blue and red areas represent the lowest and highest surface areas, respectively. However, for the PMT-processed Ti powder, an obvious macro-undulating morphology was observed for both the 45–106 μm (Fig. 7c1–7c3) and 45–75 μm (Fig. 7e1–e3) fractions, whereas a relatively smooth macro surface was obtained for the 75–106 μm fraction (Fig. 7d1–d3). In addition, from the 3D profiles, powder from 75–106 μm led to the most uniform surface topography after raking (Fig. 7d3), which is very similar to the used Arcam powder (Fig. 7b3). Although the mixed PMT-processed powder (45–106 μm) has a similar particle size distribution to the virgin Arcam powder, its performance on the powder bed was unexpected. About 57.1 vol.% of the fine particles were found in bottom areas (blue) and large particles appeared as sharp peaks (red) (Fig. 7c3), which may create excessive shear forces and then disturb the subsequent layer formation. Therefore, PMT-processed Ti powder with the size range of 75–106 μm appears to be most promising for AM when benchmarked with Arcam powder on a powder bed. The best method to test the feasibility of the powder is to build a real component by AM. A sufficient amount

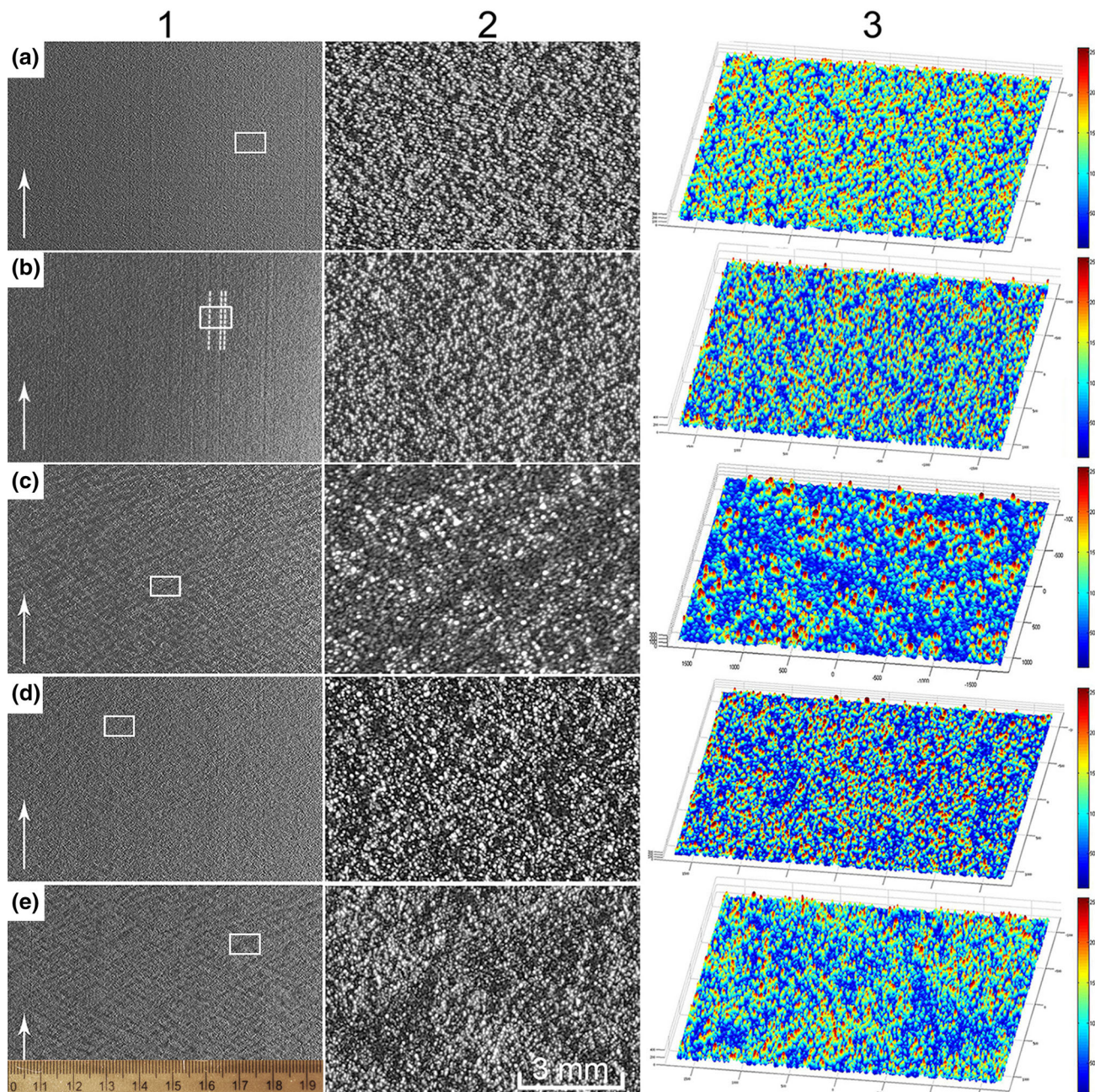


Fig. 7. Macro surface profiles of different powders raked in the UPB system: Arcam Ti-6Al-4V (a) virgin and (b) used powders, PMT-processed novel Ti powder (c) 45–106 μm , (d) 75–106 μm , and (e) 45–75 μm . The second column micrographs are enlarged topographies corresponding to each selected area (the small box) in the first column. The third column 3D profiles are converted from the second column micrographs using MATLAB. The arrows in first column show the raking direction. The three short broken lines in b1 highlight three faint rolling tracks, which are no longer visible when inspected at a high magnification (b2). The blue color and red color in the third column pictures represent the lowest and highest positions on each surface profile analyzed (Color figure online).

of the PMT-processed novel Ti powder has been produced, which will be tested in the Arcam A1 system once the processing parameters are identified. However, in the case of an insufficient volume of powder feedstock or uncertainty about the powder behavior, testing the powder in the UPB and comparing it with benchmark powder could be a rapid and efficient method to screen different powders.

CONCLUSION

A novel Ti powder precursor has been manipulated using a CSRIO proprietary technique named PMT to produce a lower cost, nearly spherical Ti powder for AM applications from feedstock that otherwise cannot be used for the AM processes due to its larger particle size and unsuitable morphology. The PMT processing of the selected novel Ti

powder precursor produced more than 50 wt.% 45–106 μm sized powder (usable for AM by EBM) and about 30 wt.% less than 45 μm sized powder (usable for AM by cold spray processes). It was identified from this study that the PMT processing of Ti sponge has the potential to produce Ti powder materials suitable for AM processes as the process is not only a cost-effective and safe size reduction method but can also effectively change particle morphology from irregular to near spherical. PMT-processed Ti powder with a size range of 75–106 μm behaved similarly in an Arcam Ti-6Al-4V powder bed compared to used Arcam Ti-6Al-4V powder. It was also identified that the UPB system can offer a quick and efficient assessment of the performance of powders prior to actual application in AM.

ACKNOWLEDGEMENTS

Y.Y. Sun acknowledges a scholarship received from the China Scholarship Council and a fee waiver scholarship offered by the RMIT University. M. Qian acknowledges the support from the Australian Research Council (ARC) through the Linkage Projects program under ARC LP140100608.

REFERENCES

1. M.J. Donachie, *Titanium: A Technical Guide* (Materials Park, OH: ASM International, 2000), p. 47.
2. L. Thijs, F. Verhaeghe, T. Craeghs, J.V. Humbeeck, and J.P. Kruth, *Acta Mater.* 58, 3303 (2010).
3. L.E. Murr, S.M. Gaytan, D.A. Ramirez, E. Martinez, J. Hernandez, K.N. Amato, P.W. Shindo, F.R. Medina, and R.B. Wicker, *J. Mater. Sci. Tech.* 28, 1 (2012).
4. L.E. Murr, S.M. Gaytan, F. Medina, M.I. Lopez, E. Martinez, and R.B. Wicker, (Paper presented at the 25th Southern Biomedical Engineering Conference 2009, Miami, FL, 2009).
5. L.E. Murr, S.A. Quinones, S.M. Gaytan, M.I. Lopez, A. Rodela, E.Y. Martinez, D.H. Hernandez, E. Martinez, F. Medina, and R.B. Wicker, *J. Mech. Behav. Biomed. Mater.* 2, 20 (2009).
6. K.P. Cooper, *JOM* 53, 29 (2001).
7. W. Xu, M. Brandt, S. Sun, J. Elambasseril, Q. Liu, K. Latham, K. Xia, and M. Qian, *Acta Mater.* 85, 74 (2015).
8. W. Xu, S. Sun, J. Elambasseril, Q. Liu, M. Brandt, and M. Qian, *JOM* 67 (2015). doi:10.1007/s11837-015-1297-8.
9. L.E. Murr, E.V. Esquivel, S.A. Quinones, S.M. Gaytan, M.I. Lopez, E.Y. Martinez, F. Medina, D.H. Hernandez, E. Martinez, J.L. Martinez, S.W. Stafford, D.K. Brown, T. Hoppe, W. Meyers, U. Lindhe, and R.B. Wicker, *Mater. Charact.* 60, 96 (2009).
10. H.P. Tang, M. Qian, N. Liu, X.Z. Zhang, G.Y. Yang, *JOM* 67 (2015). doi:10.1007/s11837-015-1300-4.
11. S.M. Gaytan, L.E. Murr, D.H. Hernandez, E. Martinez, S.A. Quinones, F. Medina, and R.B. Wicker, *Supplemental Proceedings: Vol. 1: Fabrication, Materials, Processing and Properties* (Warrendale, PA: TMS, 2009), pp. 363–369.
12. P.A. Kobryn, E.H. Moore, and S.L. Semiatin, *Scripta Mater.* 43, 299 (2000).
13. P.A. Kobryn and S.L. Semiatin, *J. Mater. Proc. Tech.* 135, 330 (2003).
14. S. Bontha, N.W. Klingbeil, P.A. Kobryn, and H.L. Fraser, *Mater. Sci. Eng. A* 513–514, 311 (2009).
15. H. Fukuda, H. Takahashi, K. Kuramoto, and T. Nakano, *Mater. Sci. Forum* 706, 488 (2012).
16. M.J. O'Hara and I.B. Cutler, *Proceedings of the British Ceramic Society*, vol. 12 (Covina, CA: SAMPE, 1969), pp. 145–154.
17. N.A. Pohlman, J.A. Roberts, and M.J. Gonser, *Powder Technol.* 228, 141 (2012).
18. A. Bauereiß, T. Scharowsky, and C. Körner, *J. Mater. Proc. Tech.* 214, 2522 (2014).
19. AMETEK Inc., *Metal-Powders*, <http://www.readingalloys.com/Products/Metal-Powders.aspx>.
20. J. Withers, J. Laughlin, and R. Loutfy (Paper presented at PM2014 World Congress, Orlando, FL, 2014).
21. X. Lu, C.C. Liu, L.P. Zhu, and X.H. Qu, *Powder Technol.* 254, 235 (2014).
22. ASTM F1877-05, Standard Practice for Characterization of Particles (West Conshohocken, PA: ASTM, 2010).
23. ASTM B855-06, Standard Test Method for Volumetric Flow Rate of Metal Powders Using Arnold Meter and Hall Funnel (West Conshohocken, PA: ASTM, 2006).
24. ASTM B703-05, Standard Test Method for Apparent Density of Powders Using Arnold Meter (West Conshohocken, PA: ASTM, 2005).
25. ASTM B527-06, Standard Test Method for Determination of Tap Density of Metallic Powders and Compounds (West Conshohocken, PA: ASTM, 2006).
26. J. Karlsson, A. Snis, H. Engqvist, and J. Lausmaa, *J. Mater. Proc. Tech.* 213, 2109 (2013).
27. Arcam AB Inc., *New! 50 μm Process for High Resolution and Surface Finish* (Mölnådal, Sweden: Arcam, 2012), <http://www.arcam.com/new-50-um-process-for-high-resolution-and-surface-finish>.
28. C. Mangano, A. Piattelli, S. d'Avila, G. Iezzi, F. Mangano, T. Onuma, and J.A. Shibli, *J. Oral. Implantol.* 36, 91 (2010).
29. C.Y. Lin, T. Wirtz, F. LaMarca, and S.J. Hollister, *J. Biol. Mater. Res. A* 83, 272 (2007).
30. T. Traini, C. Mangano, R.L. Sammons, F. Mangano, A. Macchi, and A. Piattelli, *Dental Mater.* 24, 1525 (2008).
31. A. Santomaso, P. Lazzaro, and P. Canu, *Chem. Eng. Sci.* 58, 2857 (2003).